



# Düzce University Journal of Science & Technology

Research Article

## A Study on the Physical, Optical and Radiation Shielding Capabilities of Phosphate Zinc Telluride Glasses as a Result of ZnO/In<sub>2</sub>O<sub>3</sub> Translocation

 Erkan İLİK<sup>a,\*</sup>

<sup>a</sup> Fizik Bölümü, Fen Fakültesi, Eskişehir Osmangazi Üniversitesi, Eskişehir, TÜRKİYE

\* Sorumlu yazarın e-posta adresi: [elik@ogu.edu.tr](mailto:elik@ogu.edu.tr)

DOI: 10.29130/dubited.1160535

### ABSTRACT

New In<sub>2</sub>O<sub>3</sub>-doped phosphate zinc tellurite glasses synthesized using melt-quenching method were investigated. It was observed that the synthesized glasses exhibit transparent properties. Densities of synthesized glasses changed significantly related to the doping ratio of In<sub>2</sub>O<sub>3</sub>. This implies that radiation shielding abilities can be enhanced. In other respects, the almost linear elevation in molar volume values indicated that the glass network expanded as a result of the ZnO/In<sub>2</sub>O<sub>3</sub> translocation. As the additive ratio increases, the optical band gap value increases from 2.96 eV to 3.47 eV, while the Urbach energies decrease from 0.350 eV to 0.180 eV. In<sub>2</sub>O<sub>3</sub> contribution has a regulatory effect on the structure of phosphate zinc tellurite glasses. In phosphate zinc tellurite glasses evaluated in terms of radiation shielding properties, it was observed that the In<sub>2</sub>O<sub>3</sub> additive contributed significantly to the shielding properties and the glass with the best radiation shielding was 6 mol% In<sub>2</sub>O<sub>3</sub> doped glass. It is obvious that by raising the density values of the produced glasses, the ZnO/In<sub>2</sub>O<sub>3</sub> translocation in phosphate zinc tellurite glasses enhanced their radiation shielding properties.

**Keywords:** Tellurite glasses, ZnO, In<sub>2</sub>O<sub>3</sub>, Optical band gap, Radiation shielding

## Fosfat Çinko Tellürit Camlarda ZnO/In<sub>2</sub>O<sub>3</sub> Yer Değişimi Sonucu Fiziksel, Optik ve Radyasyon Zırhlama Yetenekleri Üzerine Bir Çalışma

### Öz

Eritme-tavlama yöntemi ile sentezlenen yeni In<sub>2</sub>O<sub>3</sub> katkılı çinko fosfat tellürit camların özellikleri incelenmiştir. Sentezlenen camların saydam oldukları gözlemlenmiştir. Sentezlenen cam yoğunlukları, In<sub>2</sub>O<sub>3</sub>'ün katkı oranına bağlı olarak önemli ölçüde değişmiştir. Bu da radyasyon koruma yeteneklerinin geliştirilebileceği anlamına gelir. Öte yandan, molar hacim değerlerindeki neredeyse lineer artış, ZnO/In<sub>2</sub>O<sub>3</sub> yer değişimi sonucunda cam ağının genişlediğini göstermektedir. In<sub>2</sub>O<sub>3</sub> katkı oranı arttıkça optik bant aralığı değeri 2,96 eV'den 3,47 eV'ye yükselirken, Urbach enerjileri 0,350 eV'den 0,180 eV'ye düşmektedir. In<sub>2</sub>O<sub>3</sub> katkısının fosfat çinko tellürit camlarının yapısını düzenleyici etkisi vardır. Radyasyon zırhlama özellikleri açısından değerlendirilen fosfat çinko tellürit camlarda In<sub>2</sub>O<sub>3</sub> katkısının bu özelliklere önemli katkı sağladığı ve en iyi radyasyon zırhlama özelliğine sahip camın %6 mol In<sub>2</sub>O<sub>3</sub> katkılı cam olduğu görülmüştür. Fosfat çinko tellürit camlarındaki ZnO/In<sub>2</sub>O<sub>3</sub> yer değiştirmesi ile üretilen camların yoğunluk değerlerinin artırılarak radyasyon zırhlama özelliklerinin geliştirilebileceği söylenebilir.

## **I. INTRODUCTION**

Every living creature on earth has been continually affected by cosmic rays from the universe and radiation released by natural radioactive sources in the earth since the beginning of human history, and they coexist with natural radiation. That's why the idea of high-dose radiation has long been one of humanity's most serious threats. It is well known to everyone that various precautions should be taken to be protected from the radiation source. For this reason, various shielding materials are needed to minimize/eliminate the effects of radiation used in experimental studies or in the medical field. One of these materials is glass, which can be synthesized with very important properties in scientific studies. Glasses synthesized with different oxidized compounds naturally show different properties. Phosphate glasses are among the glass structures that are frequently used in glass science and other related fields of study. Glasses synthesized with P<sub>2</sub>O<sub>5</sub> have low glass transition temperature, and crystallization temperature decreases proportionally with the increase in the glass structure of P<sub>2</sub>O<sub>5</sub>, as well [1], [2]. Due to these important properties they bring to the glass structure, phosphate glasses are preferred in technologically important application areas such as biomedical and low-temperature cofired ceramic technology [3-5].

The ability to synthesize glasses at low melting temperatures is an important advantage for glass science and technologies. At this point, one of the element oxides preferred in many studies with its low melting temperature is TeO<sub>2</sub> glasses [6]. Instead of glass synthesis at high melting temperatures, such as borate glasses, tellurite glasses can mostly be produced below 1000 °C [7-9]. Because this crucial feature is a key aspect in the production of tellurite glasses, tellurite-based glasses are a strong candidate in literature studies and technological investigation. Tellurite glasses are popular in various applications, including optical communication networks, infrared and nonlinear applications or industrial applications as a supercontinuum generator [10-12]. In other respects, it has been reported in some studies that ZnO doped glasses show semiconducting properties. In these glass structures with different compositions, ZnO can stabilize the glass structure. There are studies in which this type of glass is used in biomaterial applications [13].

When looking at research in the subject of glass science, there are relatively few that look into the impacts of In<sub>2</sub>O<sub>3</sub> on glass [14]. In<sub>2</sub>O<sub>3</sub> is commonly utilized in thin film studies produced by various processes, whereas nanoparticles are commonly employed in glass synthesis research [15-17]. The very high density value of In<sub>2</sub>O<sub>3</sub> (7.18 g cm<sup>-3</sup>) can significantly improve the physical properties of new and unique glass structures to be synthesized. At this point, it becomes important to examine how these properties change by producing unique glass structures in which radiation shielding properties can be improved. The use of oxidized compounds with relatively high densities such as TeO<sub>2</sub> and ZnO in the glass composition would provide the desired properties to the new types of glasses to be synthesized. In addition to the physical properties of P<sub>2</sub>O<sub>5</sub>·TeO<sub>2</sub>·ZnO glass structures such as color and both experimental and theoretical radiation shielding properties have been currently studied in the literature [18-20]. There has been very few research on the impact of In<sub>2</sub>O<sub>3</sub> on glasses that have been doped [14], [17], [21]. In this study, In<sub>2</sub>O<sub>3</sub> was doped to the phosphate zinc telluride glass structure previously synthesized in the literature to improve the physical optics and especially the radiation shielding properties. It is primarily aimed to increase the density values of the glasses synthesized as a result of the translocation of ZnO with In<sub>2</sub>O<sub>3</sub>. The changes in the molar volume, density values, and optical properties of the newly synthesized glasses as well as the radiation shielding properties were investigated using WinXcom software [22].

## II. MATERIAL & METHODS

In<sub>2</sub>O<sub>3</sub> doped glasses with a nominal composition of 20P<sub>2</sub>O<sub>5</sub>·30TeO<sub>2</sub>·(50-x)ZnO·xIn<sub>2</sub>O<sub>3</sub> (x = 2, 4, 6 mol%) were prepared with oxide forms of chemicals using a digital scale. After weighing the high purity chemicals (Alfa Aesar, 99.5+%), they were taken into the sample container and mixed mechanically before melting. Then, aforementioned mixtures were taken into a porcelain crucible and placed in a high temperature furnace (Nabertherm) separately. The high temperature furnace was heated from room temperature to 900 °C for 60 min. After melting process, melted glasses were poured into a stainless steel mould and annealed at 385 °C for 60 min with another furnace (Nevola Reis 110/6) in order to minimize cracking. Synthesized glasses were coded as PTZI2 (2 mol %), PTZI4 (4 mol %), and PTZI6 (6 mol %) related to the mol % ratio. In order to obtain the optical properties of the synthesized glasses, both surfaces of the glasses were polished via Metkon Forcipol 1V and Metkon Forcimat. Photographs of the prepared glasses are given in Figure 1.



*Figure 1. Successfully synthesized In<sub>2</sub>O<sub>3</sub> doped phosphate zinc tellurite glasses*

After the glass synthesis processes were completed, the following analyzes were carried out. First of all, physical properties of these novel glasses, such as density and molar volume were calculated. Optical band gap and Urbach energy values were obtained by transmittance spectra taken over the samples within the wavelength range of 200–1100 nm. In addition, transmittances via scanning surface were determined by using different regions of the glass surface. Finally, radiation shielding parameters such as mean free path, half and tenth value layer, and effective atomic number were calculated in the next section. Gerward et al. created the WinXcom program, which is used to calculate the MAC parameter, and it may be employed in the shielding and dosimetric applications [22]. This software can rapidly and correctly calculate the MAC for any material at various energies (between 1 keV and 100 GeV), as well. In this study, broad photon energy ranges in the range of 0.01 MeV – 10 MeV were used for the aforementioned glass materials.

## III. RESULTS AND DISCUSSION

### **A. PHYSICAL PROPERTIES OF PTZI GLASSES**

Density values of synthesized glass ( $\rho_g$ ) series were calculated using Archimedes' principle. For this process, methanol with a density ( $\rho_l$ ) of 0.793 g cm<sup>-3</sup> was used as an immersion liquid. Samples were weighed first in air environment and then in the immersion liquid, respectively. Using the aforementioned principle with the help of the measured weights, the densities can be calculated with the help of the following equation [23]:

$$\rho_g = \frac{W_a}{W_a - W_l} \times \rho_l \quad (1)$$

Here,  $W_a$  and  $W_l$  represent the weight of the synthesized glasses in air and in the immersion liquid, respectively. Accordingly, calculated density values of the glasses are given in Table 1. The density value obtained after precision weighing separately in air and liquid, and the molar volume of the glasses can be calculated using the equation below:

$$V_m = \frac{\sum_i x_i M_i}{\rho_g} \quad (2)$$

**Table 1.** Density and molar volume values of  $\text{In}_2\text{O}_3$  doped phosphate zinc tellurite glasses

<b>Sample Code</b>	<b>Density (<math>\rho_g</math>) (<math>g\ cm^{-3}</math>)</b>	<b>Molar Volume (<math>V_M</math>) (<math>cm^3\ mol^{-1}</math>)</b>
PTZI2	4.51133	33.08848
PTZI4	4.55608	33.62498
PTZI6	4.60293	33.78193

In Figure 2, the density values of aforementioned glasses were in an almost linear trend depending on  $\text{In}_2\text{O}_3$  contribution ratio. The increasing molecular weight of  $\text{In}_2\text{O}_3$  doped into the  $\text{P}_2\text{O}_5 \cdot \text{TeO}_2 \cdot \text{ZnO}$  glass network increased the density values of the produced glasses as the amount of ZnO in the glass composition gradually decreased. Thus, the reason for the increase in density can be clarified by molecular weights of the translocated chemical compounds. Hereby, ZnO ( $M_w(\text{ZnO})=81.38\ g\ mol^{-1}$ ) has a lower molecular weight than  $\text{In}_2\text{O}_3$  ( $M_w(\text{In}_2\text{O}_3)=277.64\ g\ mol^{-1}$ ). As an outcome, the density values of the produced glasses have increased related to the doping ratio of  $\text{In}_2\text{O}_3$ . Similar studies showed that the determined density values in accordance with the literature [14].

As is known, molar volume is defined as the volume of one mole of a material. PTZI2, PTZI4, and PTZI6 glasses have molar volumes of  $33.08848\ cm^3\ mol^{-1}$ ,  $33.62498\ cm^3\ mol^{-1}$ , and  $33.78193\ cm^3\ mol^{-1}$ , respectively. In this study, molar volume values increase as a result of the contribution of  $\text{In}_2\text{O}_3$ . The molar volume value first showed a sharp increase when the  $\text{In}_2\text{O}_3$  additive ratio was increased from 2 mol% (PTZI2) to 4 mol% (PTZI4). As a result of increasing the contribution rate to 6 mol% (PTZI6), it continued to increase in a similar manner. However, this increase was less than the previous change. The increase in molar volume can be explained by the expansion of the glass network depending on the  $\text{In}_2\text{O}_3$  doping ratio. ZnO/ $\text{In}_2\text{O}_3$  translocation in glasses allowed larger structures to enter the glass network and increased the number of moles per unit volume. Furthermore, as shown in Figure 1, physical imperfections in  $\text{P}_2\text{O}_5 \cdot \text{TeO}_2 \cdot \text{ZnO}$  glasses may be removed by including  $\text{In}_2\text{O}_3$  in the glass network.

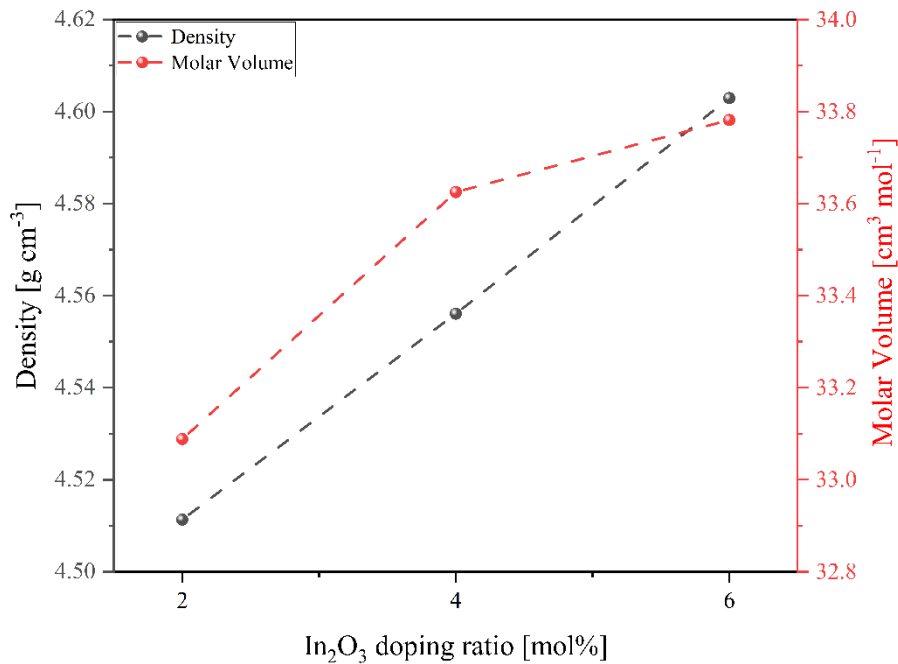


**Figure 2.** Density and molar volume value changing of In<sub>2</sub>O<sub>3</sub> doping ratio. Dashed lines to guide the eye.

## B. OPTICAL PROPERTIES OF PTZI GLASSES

Optical characterization data such as transmittance, optical band gap, and Urbach energies of P<sub>2</sub>O<sub>5</sub>·TeO<sub>2</sub>·ZnO/In<sub>2</sub>O<sub>3</sub> samples were obtained using transmittance and absorption spectra in the range of 190-1100 nm. In order to determine the defects of the samples synthesized with ZnO/In<sub>2</sub>O<sub>3</sub> translocation, optical surface transmittances were taken with Analytik Jena Specord 210 plus device as scanning. Figure 3, Figure 4, and Figure 5 show the scan transmittance spectra taken over the surfaces of the synthesized samples. Instead of collecting a single region, the surface scanning approach was used to collect a total of 36 measurements from 1 cm of the sample to draw the transmittance spectra. However, the absorption edge had the same characteristics throughout all sample spectra. When the spectra of the samples were compared based on In<sub>2</sub>O<sub>3</sub> alteration, the rise in In<sub>2</sub>O<sub>3</sub> changed the absorption edge to blue-region (blue shift). In the visible region, each sample had a transmittance of more than 80%. The optical band gap changes due to the shift in the absorption edge. The optical band gap was computed using Tauc technique [24]. Figure 6 (a) illustrates the Tauc curves that were utilized to calculate the optical band gap and Figure 6 (b) presents all of the  $\ln\alpha \sim h\nu$  graphs for Urbach energies. When the obtained values were evaluated, the optical band gap increased due to the ZnO/In<sub>2</sub>O<sub>3</sub> adjustment. The widest optical band gap value was found with 6 mol percent In<sub>2</sub>O<sub>3</sub> doped glass sample, and optical band gap values ranged from 2.96 eV to 3.47 eV. In a literature study, the optical properties of TeO<sub>2</sub>·ZnO·In<sub>2</sub>O<sub>3</sub> shows a similar trend [14]. The optical band gap widens as In<sub>2</sub>O<sub>3</sub> concentration rises. This demonstrates how the current study as well as the literature are consistent. The increase in NBOs and the more ionic nature of the structure account for the decrease in optical band gap value with the addition of a new element [25], [26]. Urbach energy indicates the uniformity and stability of comparable glass formations. If the Urbach energy of the synthesized glasses is reduced by an additive, the aforementioned glass structures can be interpreted as being so stable and uniform. The most irregular structure in the synthesized samples was revealed to be PTZI2 with 2 mol% In<sub>2</sub>O<sub>3</sub> additive, while the most stable structure belonged to PTZI6 with 6 mol% In<sub>2</sub>O<sub>3</sub> additive. As a result, the ZnO/In<sub>2</sub>O<sub>3</sub> translocation improves the structure as a more stable. The Urbach energies in TeO<sub>2</sub>·ZnO·In<sub>2</sub>O<sub>3</sub> have been observed to climb to a certain level and subsequently fall [14]. Although the optical band gap values for this structure reported in the literature correspond with the based on the specified in this work, the variation in Urbach energies can be attributed to variances in the glass network, which does not match. The increase in the In<sub>2</sub>O<sub>3</sub> ratio eliminates the negative effects such as fluctuations and undesirable colorations in the synthesized glass. As seen before in Figure 1, it provides the glass structure more orderly. This phenomenon is seen in the 3D surface transmittance graphs using the transmittance curves

taken from 36 different regions of the glass surface. In addition, the decrease in the Urbach energy with the increase in  $\text{In}_2\text{O}_3$  can be shown as proof of this phenomenon (see Table 2).

**Table 2.** Optical band gap and Urbach energy values of  $\text{In}_2\text{O}_3$  doped phosphate zinc tellurite glasses with fitting parameter ( $R^2$ )

Sample Code	Optical Band Gap (eV)	Equation	$R^2$	Slope	Urbach Energy (eV)
PTZI2	2.96	$y=-3.9073+2.8542*x$	0.9989	2.8542	0.350
PTZI4	3.15	$y=-5.2738+3.1665*x$	0.9979	3.1665	0.316
PTZI6	3.47	$y=-14.6712+5.5499*x$	0.9974	5.5499	0.180

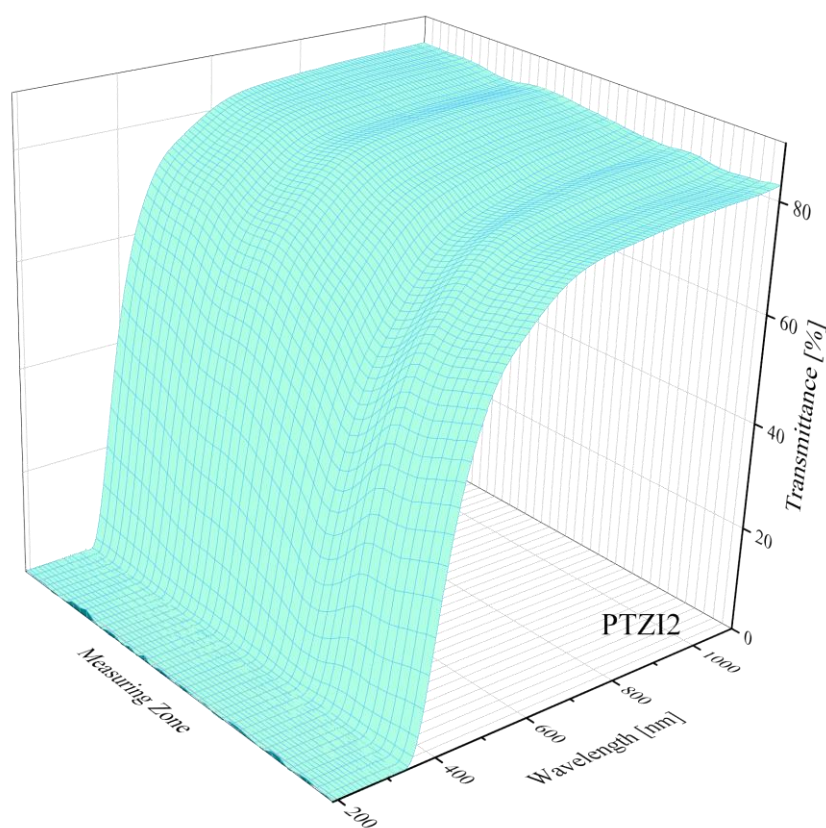


**Figure 3.** Three-dimensional surface transmittance scanning for PTZI2 sample

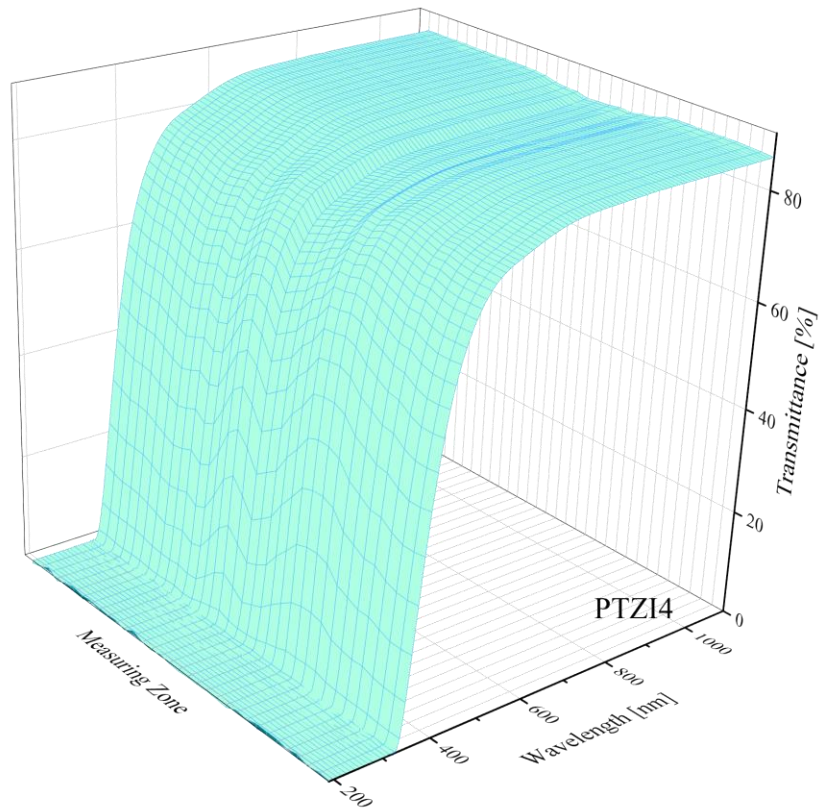


**Figure 4.** Three-dimensional surface transmittance scanning for PTZI4 sample

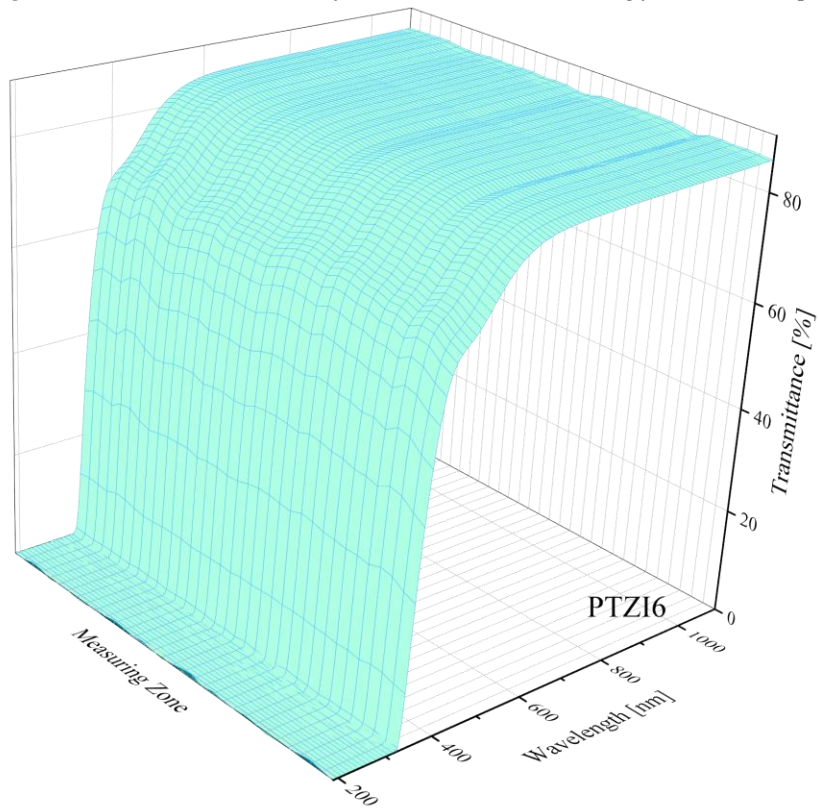


**Figure 5.** Three-dimensional surface transmittance scanning for PTZI6 sample

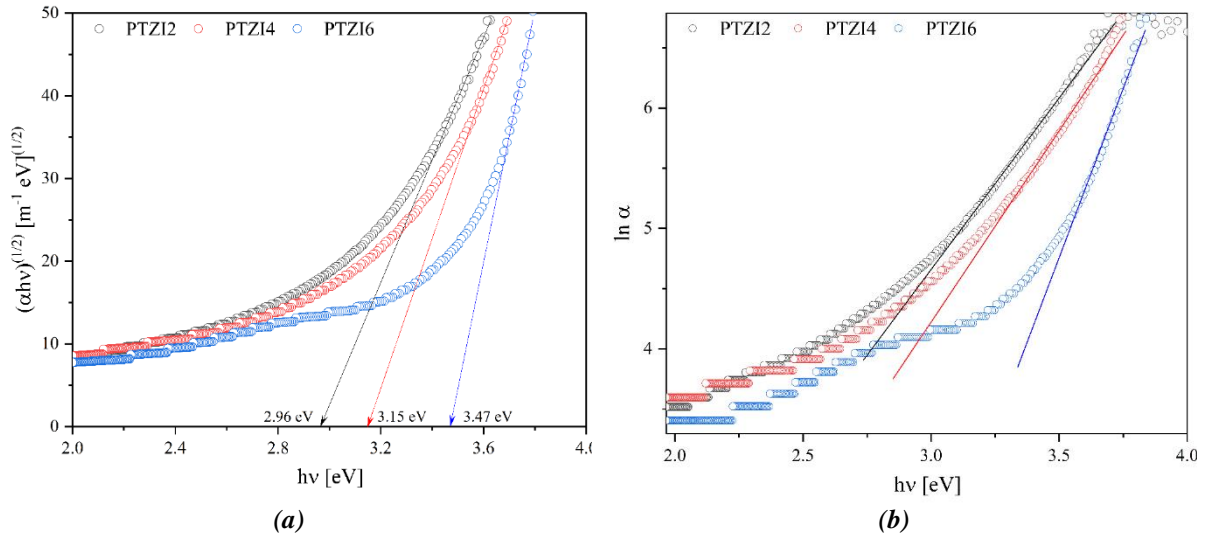


**Figure 6.** (a) Optical band gap and (b) Urbach energy values of  $In_2O_3$  doped phosphate zinc tellurite glasses

### C. RADIATION SHIELDING PROPERTIES OF PTZI GLASSES

In order to determine radiation shielding properties of materials, WinXcom database is a great alternative for manual computations using tabular data. This web-based database may be used to compute radiation shielding properties for the material being examined. Since then, the National Institute of Standards and Technology (NIST) has created a tool called Xcom to calculate the mass attenuation coefficients for any element, compound or mixture. The Lambert-Beer equation governs the transmission fraction of a beam of monochromatic radiation in a medium. Glass samples are used as the medium through which the incoming photons pass. According to this rule, the amount of absorbed radiation is first proportional to the photon's travel length through the medium and then the density of the medium [27]:

$$I = I_0 e^{-\mu t} \quad (3)$$

Here,  $I_0$  represents the incident photons intensity.  $\mu$  and  $t$  are the linear attenuation coefficient (LAC) and thickness of the glass samples, respectively. Accordingly, Figure 7 (a) depicts the variations in linear attenuation coefficients obtained for the synthesized glasses as a function of energy varied from 0.01 MeV to 10 MeV.

When these changes are analyzed, the glass with the greatest LAC value in all energy ranges is the 6 mol%  $In_2O_3$  doped PTZ6 sample. On the other hand, when the LAC values of the synthesized glasses are compared among themselves and all energy regions are considered, it can be said that the  $ZnO/In_2O_3$  translocation has an increasing effect on the LAC values of the synthesized glass samples, as well. On the other hand, the increase in energy causes a decrease in LAC values for all samples and a similar trend is observed for all synthesized glass structures.

The mass attenuation coefficient of a sample whose linear attenuation coefficient is known can be calculated with the following equation [27]:

$$MAC = \frac{LAC}{\rho_g} = \mu_{\rho_g} = \sum_i W_i \mu_i \rho_i \quad (4)$$

The mass attenuation coefficient (also called as the mass absorption coefficient) is a constant that defines the proportion of photons eliminated per unit mass from a monochromatic X- or  $\gamma$ -ray beam by a

homogeneous absorber. The MAC computations were carried out between 0.01 MeV and 10 MeV as can be given in Figure 8 (b). In order to calculate mass attenuation coefficient of any sample, the density values of the samples ( $\rho_g$ ) are used and these values were included in Table 1. The sequence of MAC values is PTZI6>PTZI4>PTZI2 from biggest to smallest, as in the linear attenuation graph. For example, the MAC values for PTZI2, PTZI4 and PTZI6 at 0.1 MeV energy were calculated as 0.7086 cm<sup>2</sup> g<sup>-1</sup>, 0.7272 cm<sup>2</sup> g<sup>-1</sup> and 0.9604 cm<sup>2</sup> g<sup>-1</sup>, respectively. The dramatically fall in MAC values in the lowest energy zone is attributed to the photoelectric absorption coefficient's dominance. The findings demonstrate that the MAC varies with energy in the same manner in all of the glasses. It was noticed that the MAC values were highest when there was the least amount of energy and rapidly decreased as energy increased.

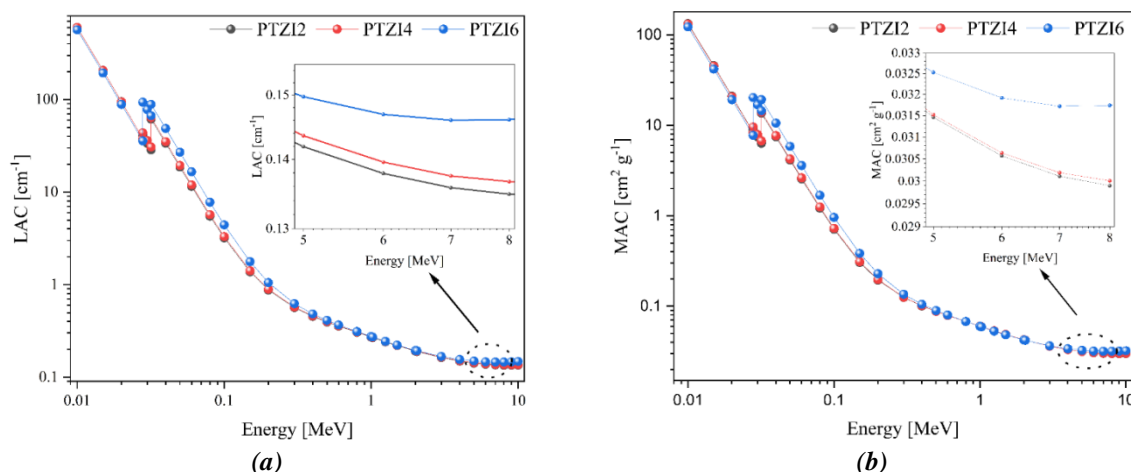


**Figure 7.** Variations of (a) LAC and (b) MAC of PTZI glasses with changing of energy ranges varying from 0.01 MeV to 10 MeV

The Compton scattering absorption mechanism is responsible for the steady drop in this coefficient. Photons are lost to the Compton scattering process by colliding inelastically with free electrons in the interaction medium. The absorption of Compton interactions is inversely proportional to photon energy. The pair production absorption process occurs at 6 MeV and dominates the mass attenuation cross section's behavior. The total pair formation cross section has a threshold energy of 1.022 MeV, rises with photon energy, and becomes significant above 10 MeV.

The average thickness of the glass necessary to absorb 90% and 50% of all X- and  $\gamma$ -rays is important for shielding applications. These are well known as the tenth and half value layer (*TVL*) and (*HVL*) and calculated using linear attenuation coefficient values. It is vital to note that the lower the glass sample's *HVL* and *TVL*, the higher the X- and  $\gamma$ -ray shielding efficiency. These two parameters are represented in distance units (cm), and they can be calculated using the following equations [28]:

$$HVL = \frac{\ln 2}{LAC} \quad (5)$$

$$TVL = \frac{\ln 10}{LAC} \quad (6)$$

Figure 8 shows the variation of half and tenth value layers of PTZI glasses with increasing energy from 0.01 MeV to 10 MeV. *TVL* and *HVL* increased with the increase in penetration energy. As it is well known, secondary photons are produced via incoherent scattering and pair production interaction processes at higher photon energies. As a consequence, extra material thickness is required to absorb these secondary photons. For *HVL* and *TVL*, it can be said that the ZnO/In<sub>2</sub>O<sub>3</sub> translocation gains better features to the base glass structure. When examining the changes in *HVL* and *TVL*, it is clear that the radiation shielding properties of glass structures can be improved with the addition of In<sub>2</sub>O<sub>3</sub>.

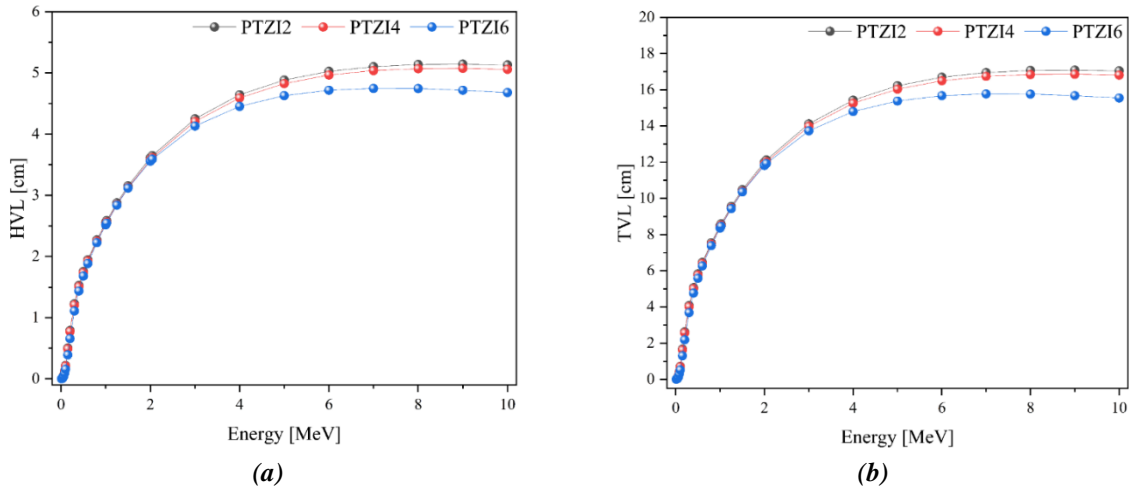


**Figure 8.** Variations of (a) HVL and (b) TVL of PTZI glasses with changing of energy ranges varying from 0.01 MeV to 10 MeV

The average distance traveled by photons between collisions is referred to as the mean free path (*MFP*). The *MFP* can be calculated using the linear attenuation coefficient from the following equation [23]:

$$MFP = \frac{1}{LAC} \tag{7}$$

Because the *MFP* for high density materials is relatively short, the materials can be utilized as an effective material against X- and gamma-rays. According to the findings, the PTZI2 sample with the lowest In<sub>2</sub>O<sub>3</sub> content had the highest mean free path values for all incident photon energy (as can be seen in Figure 9). In other respects, the fact that the mean free path has decreased in the PTZI6 sample is evidence of its superior characteristics. It is obvious that when the density of the material increased from 4.51133 g cm<sup>-3</sup> to 4.60293 g cm<sup>-3</sup>, the mean free path in the glass structure decreased. Based on the literature, different glass compositions containing In<sub>2</sub>O<sub>3</sub> are consistent with this study [14].

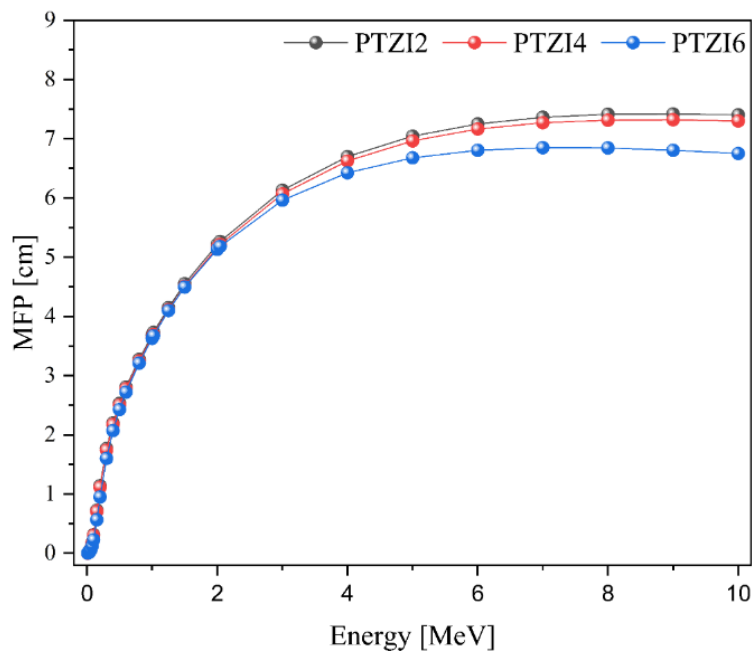


**Figure 9.** Variations of MFP of PTZI glasses with changing of energy ranges varying from 0.01 MeV to 10 MeV

The effective atomic number ( $Z_{eff}$ ) of photons in a medium can be used to evaluate the interaction between photons and the medium. It is a number that, like an element's atomic number, defines the chemical description of a composite substance. Yet, unlike the atomic number, this is not constant and evolves with photon energy [29]. The  $Z_{eff}$  value of structures containing atoms of more than one element, such as glass or composite, may be computed using the following equation [23]:

$$Z_{eff} = \frac{\sum_i f_i A_i \left(\frac{\mu}{\rho}\right)_i}{\sum_j f_j \left(\frac{A}{Z}\right)_j \left(\frac{\mu}{\rho}\right)_j} \quad (8)$$

Accordingly, Figure 10 shows the variations of  $Z_{eff}$  of PTZI glasses with changing of energy ranges varying from 0.01 MeV to 10 MeV. First, the  $Z_{eff}$  values of the PTZI samples in the low energy region first formed a sharp peak. This peak follows the same trend for all glasses. In the photoelectric area,  $Z_{eff}$  is significantly reliant on the sample composition [28]. When the energy value of the incident photons increased up to 1.5 MeV, the  $Z_{eff}$  value decreased gradually, and then continued to increase up to a certain point. To summarize, it can be said that PTZI6 comes to the fore in all photon energies and as a result of this study, it can be said that the effective atomic number range for the glass composition is between Cu( $Z=29$ ) and Pd( $Z=46$ ).

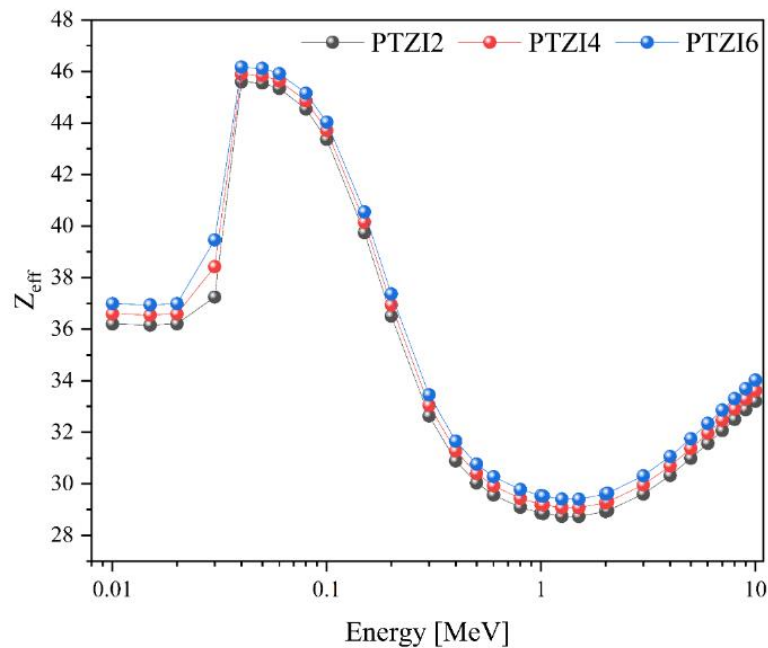


**Figure 10.** Variations of  $Z_{eff}$  of PTZI glasses with changing of energy ranges varying from 0.01 MeV to 10 MeV

## IV. CONCLUSIONS

In this study, the effects of ZnO/ $\text{In}_2\text{O}_3$  translocation on phosphate zinc tellurite glasses are discussed in terms of changes in physical, optical, and radiation shielding properties. As a physical examination, the density values of the three glass samples increased from  $4.51133 \text{ g cm}^{-3}$  to  $4.60293 \text{ g cm}^{-3}$  with the contribution of  $\text{In}_2\text{O}_3$ . ZnO/ $\text{In}_2\text{O}_3$  translocation caused an increase in the molar volume values of PTZI glasses and thus the expansion of the glass network. On the other hand, it was observed that the ZnO/ $\text{In}_2\text{O}_3$  translocation significantly increased the optical band gap values of the synthesized glasses and decreased the Urbach energy values. Furthermore, the increase in the  $\text{In}_2\text{O}_3$  ratio eliminates the negative effects such as undesirable colorations in the synthesized samples. It can be mentioned when the produced samples are assessed in terms of radiation shielding properties, the ZnO/ $\text{In}_2\text{O}_3$  translocation

for *HVL* and *TVL* offers to the basic glass structure improved qualities. The PTZI6 sample's mean free path value reduced and its radiation shielding capacity rose, both of which are strikingly correlated with the  $\text{In}_2\text{O}_3$  contribution rate. As the densities of the manufactured glasses grow, so does the effective atomic number. Consequently, increasing densities of  $\text{ZnO}/\text{In}_2\text{O}_3$  exchanged PTZ glasses demonstrate promising radiation shielding performance. It is obvious that doping denser element oxides to comparable base glass frameworks will yield even better outcomes for radiation shielding applications.

## **V. REFERENCES**

- [1] M. Uo, M. Mizuno, Y. Kuboki, A. Makishima, and F. Watari, "Properties and cytotoxicity of water soluble  $\text{Na}_2\text{O}-\text{CaO}-\text{P}_2\text{O}_5$  glasses", *Biomaterials*, vol. 19, no. 24, pp. 2277–2284, 1998.
- [2] K. El-Egili, H. Doweidar, Y.M. Moustafa, and I. Abbas, "Structure and some physical properties of  $\text{PbO}-\text{P}_2\text{O}_5$  glasses", *Physica B: Condensed Matter*, vol. 339, no. 4, pp. 237–245, 2003.
- [3] M. A. Lopes, R. F. Silva, F. J. Monteiro, and J. D. Santos, "Microstructural dependence of Young's and shear moduli of  $\text{P}_2\text{O}_5$  glass reinforced hydroxyapatite for biomedical applications", *Biomaterials*, vol. 21, no. 7, pp. 749–754, 2000.
- [4] Z. Chen, X. Chen, W. Zhang, H. Mao, and F. Wang, "Sintering behavior and dielectric properties of  $\text{La}_2\text{O}_3-\text{B}_2\text{O}_3-\text{CaO}-\text{P}_2\text{O}_5$  glass/ $\text{Al}_2\text{O}_3$  composites for LTCC applications", *Journal of Materials Science: Materials in Electronics*, vol. 31, no. 21, pp. 18581–18589, 2020.
- [5] H. A. Abo-Mosallam and E. A. Mahdy, "Effect of strontium on crystallization characteristics and properties of  $\text{ZnO}-\text{Fe}_2\text{O}_3-\text{B}_2\text{O}_3-\text{P}_2\text{O}_5$  glass-ceramics for biomedical applications", *Journal of Non-Crystalline Solids*, vol. 583, 121467(pp. 1–7), 2022.
- [6] Y. Zhou, Y. Yang, F. Huang, J. Ren, S. Yuan, and G. Chen, "Characterization of new tellurite glasses and crystalline phases in the  $\text{TeO}_2-\text{PbO}-\text{Bi}_2\text{O}_3-\text{B}_2\text{O}_3$  system", *Journal of Non-Crystalline Solids*, vol. 386, pp. 90–94, 2014.
- [7] M. Farahmandjou and S. A. Salehizadeh, "The optical band gap and the tailing states determination in glasses of  $\text{TeO}_2-\text{V}_2\text{O}_5-\text{K}_2\text{O}$  system", *Glass Physics and Chemistry*, vol. 39, no. 5, pp. 473–479, 2013.
- [8] K. Kato, T. Hayakawa, Y. Kasuya, and P. Thomas, "Influence of  $\text{Al}_2\text{O}_3$  incorporation on the third-order nonlinear optical properties of  $\text{Ag}_2\text{O}-\text{TeO}_2$  glasses", *Journal of Non-Crystalline Solids*, vol. 431, pp. 97–102, 2016.
- [9] N. S. Tagiara, D. Palles, E. D. Simandiras, V. Psycharis, A. Kyritsis, and E. I. Kamitsos, "Synthesis, thermal and structural properties of pure  $\text{TeO}_2$  glass and zinc-tellurite glasses", *Journal of Non-Crystalline Solids*, vol. 457, pp. 116–125, 2017.
- [10] A. Mori, "Tellurite-based fibers and their applications to optical communication networks", *Journal of the Ceramic Society of Japan*, vol. 116, no. 1358, pp. 1040–1051, 2008.
- [11] A. Lin, A. Zhang, E. J. Bushong, and J. Toulouse, "Solid-core tellurite glass fiber for infrared and nonlinear applications", *Optics express*, vol. 17, no. 19, pp. 16716–16721, 2009.
- [12] P. Froidevaux, A. Lemièrre, B. Kibler, F. Désévéday, P. Mathey, G. Gadret, J-C. Jules, K. Nagasaki, T. Suzuki, Y. Ohishi, and F. Smektala, "Dispersion-engineered step-index tellurite fibers for mid-infrared coherent supercontinuum generation from 1.5 to 4.5  $\mu\text{m}$  with sub-nanojoule femtosecond pump pulses. *Applied Sciences*, vol. 8, no. 10, 1875(pp. 1–13), 2018.

- [13] E. A. Abou Neel, L. A. O'Dell, M. E. Smith, and J. C. Knowles, "Processing, characterisation, and biocompatibility of zinc modified metaphosphate based glasses for biomedical applications", *Journal of Materials Science: Materials in Medicine*, vol. 19, no. 4, pp. 1669–1679, 2008.
- [14] G. Kilic, E. Ilik, S. A. Issa, B. Issa, U. G. Issever, H. M. Zakaly, and H. O. Tekin, "Fabrication, structural, optical, physical and radiation shielding characterization of indium (III) oxide reinforced  $85\text{TeO}_2\text{-(15-x)ZnO-xIn}_2\text{O}_3$  glass system", *Ceramics International*, vol. 47, no. 19, pp. 27305–27315, 2021.
- [15] Y. Meng, X. L. Yang, H. X. Chen, J. Shen, Y. M. Jiang, Z. J. Zhang, and Z. Y. Hua, "A new transparent conductive thin film  $\text{In}_2\text{O}_3\text{: Mo}$ ", *Thin Solid Films*, vol. 394, no. 1–2, pp. 218–222, 2001.
- [16] A. El Hichou, A. Kachouane, J. L. Bubendorff, M. Addou, J. Ebothe, M. Troyon, and A. Bougrine, "Effect of substrate temperature on electrical, structural, optical and cathodoluminescent properties of  $\text{In}_2\text{O}_3\text{-Sn}$  thin films prepared by spray pyrolysis", *Thin Solid Films*, vol. 458, no. 1–2, pp. 263–268, 2004.
- [17] P. Chen, Y. Mao, S. Hou, Y. Chen, X. Liu, Y. Lou, A. Chen, L. Yang, N. Li, and N. Dai, (2019). Effects of  $\text{In}_2\text{O}_3$  nanoparticles doping on the photoluminescent properties of  $\text{Eu}^{2+}/\text{Eu}^{3+}$  ions in silica glasses", *Ceramics International*, vol. 45, no. 1, pp. 233–238, 2019.
- [18] T. Konishi, T. Hondo, T. Araki, K. Nishio, T. Tsuchiya, T. Matsumoto, S. Suehara, S. Todoroki, and S. Inoue, "Investigation of glass formation and color properties in the  $\text{P}_2\text{O}_5\text{-TeO}_2\text{-ZnO}$  system", *Journal of Non-Crystalline Solids*, vol. 324, no. 1–2, pp. 58–66, 2003.
- [19] E. Kavaz, E. Ilik, G. Kilic, G. ALMisned, and H. O. Tekin, "Synthesis and experimental characterization on fast neutron and gamma-ray attenuation properties of high-dense and transparent Cadmium oxide ( $\text{CdO}$ ) glasses for shielding purposes", *Ceramics International*, vol. 48, no. 16, pp. 23444–23451, 2022.
- [20] G. Kilic, E. Kavaz, E. Ilik, G. ALMisned, and H. O. Tekin, "CdO-rich quaternary tellurite glasses for nuclear safety purposes: Synthesis and experimental gamma-ray and neutron radiation assessment of high-density and transparent samples", *Optical Materials*, vol. 129, pp. 112512, pp. 1–10, 2022.
- [21] R. Garkova, G. Völksch, and C. Rüssel, " $\text{In}_2\text{O}_3$  and tin-doped  $\text{In}_2\text{O}_3$  nanocrystals prepared by glass crystallization", *Journal of Non-Crystalline Solids*, vol. 352, no. 50–51, pp. 5265–5270, 2006.
- [22] L. Gerward, N. Guilbert, K. B. Jensen, and H. Levring, (2004). "WinXCom—a program for calculating X-ray attenuation coefficients" *Radiation Physics and Chemistry*, vol. 71, no. 3-4, pp. 653–654, 2004.
- [23] E. Ilik, "Effect of heavy rare-earth element oxides on physical, optical and gamma-ray protection abilities of zinc-borate glasses", *Applied Physics A*, vol. 128, no. 6, pp. 1–10, 2022.
- [24] G. Kilic, E. Ilik, U. G. Issever, and M. Peker, "The effect of  $\text{B}_2\text{O}_3/\text{CdO}$  substitution on structural, thermal, and optical properties of new black PVB/Cd semiconducting oxide glasses", *Applied Physics A*, vol. 126, no. 7, pp. 1-12, 2020.
- [25] J. Gouteron, D. Michel, A. M. Lejus, and J. Zarembowitch, "Raman spectra of lanthanide sesquioxide single crystals: Correlation between A and B-type structures", *Journal of Solid State Chemistry*, vol. 38, no 3, pp. 288–296, 1981.

- [26] G. Kilic, E. Ilik, S. A. Issa, and H. O. Tekin, "Synthesis and structural, optical, physical properties of Gadolinium (III) oxide reinforced  $\text{TeO}_2\text{-B}_2\text{O}_3\text{-(20-x) Li}_2\text{O-xGd}_2\text{O}_3$  glass system", *Journal of Alloys and Compounds*, vol. 877, 160302, pp. 1–12, 2021.
- [27] E. Kavaz, H. O. Tekin, G. Kilic, and G. Susoy, "Newly developed Zinc-Tellurite glass system: an experimental investigation on impact of  $\text{Ta}_2\text{O}_5$  on nuclear radiation shielding ability", *Journal of Non-Crystalline Solids*, vol. 544, 120169, pp. 1–11, 2020.
- [28] E. Kavaz, "An experimental study on gamma ray shielding features of lithium borate glasses doped with dolomite, hematite and goethite minerals", *Radiation Physics and Chemistry*, vol. 160, pp. 112–123, 2019.
- [29] O. Olarinoye, "Variation of effective atomic numbers of some thermoluminescence and phantom materials with photon energies", *Research Journal of Chemical Sciences*, vol. 1, no. 2, pp. 64–69, 2011.